



Sustainable and scalable natural fiber welded palladium-indium catalysts for nitrate reduction



David P. Durkin^{a,1,2}, Tao Ye^{b,1,3}, Jonglak Choi^{c,4}, Kenneth J.T. Livi^{d,7}, Hugh C. De Long^{e,6}, Paul C. Trulove^{f,5}, D. Howard Fairbrother^{a,2}, Luke M. Haverhals^{g,*}, Danmeng Shuai^{b,**}

^a Department of Chemistry, Johns Hopkins University, Baltimore, MD, 21218, United States

^b Department of Civil and Environmental Engineering, The George Washington University, Washington, DC, 20052, United States

^c Natural Fiber Welding Incorporated, Peoria, IL, 61625, United States

^d Department of Materials Science and Engineering, Johns Hopkins University, Baltimore, MD, 21218, United States

^e U. S. Army Research Office, Research Triangle Park, NC, 27709, United States

^f Department of Chemistry, U. S. Naval Academy, Annapolis, MD, 21401, United States

^g Department of Chemistry and Biochemistry, Bradley University, Peoria, IL, 61625, United States

ARTICLE INFO

Keywords:

Palladium
Indium
Nitrate
Natural fiber welding

ABSTRACT

In this work, we demonstrate the production of reactive, robust, sustainable catalysts for water treatment created through *Natural Fiber Welding* (NFW) of lignocellulose-supported palladium-indium (Pd-In) nanoparticles onto linen yarns. First, Pd-In catalysts were synthesized by incipient wetness onto ball-milled powders of linen. Our process preserved the lignocellulose, yielding small (5–10 nm), near-spherical crystalline nanoparticles of Pd-In alloy and a uniform Pd-In metal composition throughout the fibers. Nitrate reduction tests identified the existence of an optimum Pd-In catalyst composition (5 wt% Pd and 1.2 wt% In with respect to lignocellulose) for maximum reactivity; the most reactive Pd-In catalyst was 10 times more reactive than the best performing Pd-Cu nanoparticles deposited on lignocellulose using the same approach. This improved performance was most likely due to more uniform distribution of alloyed Pd-In nanoparticles throughout the support. Nitrate reduction tests and X-ray photoelectron spectroscopy depth profiling of aged Pd-In catalysts showed that they remained stable and lost no reactivity during extended storage in air at room temperature. Next, the optimized Pd-In catalyst was fiber-welded onto linen yarns, using a custom-built yarn-coating system and a novel, scalable process that controlled catalyst loading, delivering a Pd-In catalyst coating onto the yarn surface. This fiber-welded Pd-In catalyst yarn was integrated into a novel water treatment reactor and evaluated during four months and more than 180 h of nitrate reduction tests in ultrapure water. During this evaluation, the fiber-welded catalysts maintained their reactivity with negligible metal leaching. When tested in raw or (partially) treated drinking water and wastewater, the fiber-welded catalysts were robust and stable, and their performance was not significantly impacted by constituents in the complex waters (e.g. alkalinity, organic matter). Our research demonstrates an innovative, scalable approach through NFW to design and implement robust, sustainable lignocellulose-supported catalysts with enhanced reactivity capable of water purification in complex water chemistries.

* Corresponding author at: Bradley University, Department of Chemistry, 1501 W Bradley Avenue, Peoria, IL 61625, United States.

** Corresponding author at: The George Washington University, Department of Civil and Environmental Engineering, 800 22nd St NW, Suite 3530, Science and Engineering Hall, Washington, DC 20052, United States.

E-mail addresses: lhaverhals@fsmail.bradley.edu (L.M. Haverhals), danmengshuai@gwu.edu (D. Shuai).

¹ Equal contribution.

² Johns Hopkins University, Department of Chemistry, 3400 N. Charles Street, Baltimore, MD 21218, United States.

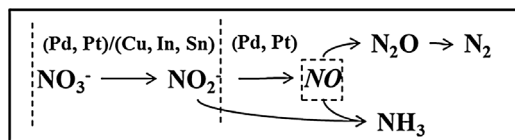
³ The George Washington University, Department of Civil and Environmental Engineering, 800 22nd St NW, Suite 3530, Science and Engineering Hall, Washington, DC 20052, United States.

⁴ Natural Fiber Welding, Inc. 801 W. Main St. Peoria, IL 61606, United States.

⁵ United States Naval Academy, Department of Chemistry, 572 M Holloway Rd, Annapolis, MD 21402, United States.

⁶ U. S. Army Research Office, 800 Park Office Drive, Suite #4229, Research Triangle Park, NC 27709, United States.

⁷ Johns Hopkins University, Department of Materials Science and Engineering, 3400 N. Charles St, Baltimore, MD 21218, United States.



Scheme 1. Nitrate reduction pathway on noble metal-based catalysts, with NO as a proposed intermediate.

1. Introduction

Nitrate is a persistent contaminant in surface water and groundwater [1], generated from extensive agricultural practices, industrial processes, and improper septic disposal [2–4]. Its contamination causes ‘blue baby syndrome’ [5], as well as the production of carcinogenic *N*-nitroso compounds in human bodies [6,7]. To mitigate the health impact of nitrate contamination in drinking water, the World Health Organization (WHO) and U.S. Environmental Protection Agency (USEPA) have established guidelines or maximum contaminant levels (MCLs) for nitrate: 50 mg L⁻¹ (WHO) [8] and 10 mg L⁻¹ as N (USEPA) [9], respectively. Reverse-osmosis and ion exchange are the conventional methods to physically remove nitrate; however, these methods result in concentrated brine that requires further treatment or disposal. Biological denitrification (e.g., biological granular activated carbon treatment) has also been used for nitrate removal in drinking water purification, however the public has concerns with increased pathogen growth, turbidity, disinfectant demand, and the likelihood of disinfection byproduct formation in the treated water [10]. Noble metal-based catalytic hydrogenation has emerged as a promising strategy to chemically reduce nitrate, as described in reaction Scheme 1 [11–15]. Not only does it use a clean reducing agent, H₂, which can yield minimal byproducts during nitrate treatment, but noble metal-based catalysts can be regenerated and reused, and the hydrogenation process can potentially be engineered for industrial scale implementation with a reduced cost and environmental impact [15–18].

Nitrate reduction to nitrite requires a noble metal (e.g., palladium (Pd), platinum (Pt)) in close proximity or direct contact with a promoter metal (e.g., copper (Cu), indium (In), tin (Sn)). During reduction, an oxygen atom of nitrate is transferred to the promoter metal, which is subsequently reduced by atomic hydrogen dissociated by the noble metal, and the intermediate nitrite is formed. The reduction of nitrite and subsequent N-containing species (e.g., N₂O), requires only the noble metal and dissociated atomic hydrogen [19]. Many studies have shown how the choice of promotor metal (i.e., Cu [14,20–22], In [23–27], or Sn [27]) can significantly impact catalyst performance.

To be useful in practical water treatment applications, bimetal catalysts need to be immobilized onto a supporting material. Conventional catalyst supports (i.e., alumina [28], silica [29,30], titanium dioxide [31], and activated carbon [32]) have been extensively studied due to their high surface areas and favorable performance. However, these conventional supports are most often used as highly dispersed powders and are difficult to transport or recover. When these supported catalysts (in the form of larger, millimeter-sized, porous particles/pellets) are used for continuous flow reactor designs, they often exhibit lower reactivity due to aqueous-solid mass transfer limitations and/or gas-liquid mass transfer limitations of H₂ [17,33]. Finally, these conventional catalyst supports can have costly production or recycling processes that negatively impact the environment [34,35]. To meet these challenges, more sustainable alternatives to conventional catalyst supports are required.

Lignocellulose fibers are earth-abundant, natural materials that are inexpensive to fabricate, and hold great promise as catalyst supports because they are rich in surface functional groups (e.g., –OH, –C–O–C–) that promote nanoparticle deposition and dispersion. Previous studies have shown how single-metal catalytic nanoparticles (i.e., Pt, Pd, Cu, gold (Au), or silver (Ag)) can be grown on cellulose [36–39]. Most

recently, our lab successfully loaded bimetal Pd–Cu nanoparticles on lignocellulose fibers (i.e., linen and bamboo) and applied them to the catalytic hydrogenation of nitrate [40]. We further demonstrated how *Natural Fiber Welding* (NFW) [41] could transform the lignocellulose-supported Pd–Cu catalyst into a free-standing, moldable structure for water treatment. The ability to be post-processed through NFW is a distinct advantage lignocellulose has over conventional catalyst supports. In contrast to catalysts on conventional supports, lignocellulose-supported catalysts can be engineered through NFW in a sustainable manner to facilitate catalyst recovery, regeneration, and reuse. Our current research stems from motivation to leverage this engineering advantage and design reactive, scalable, sustainable catalytic systems for water purification.

In NFW, lignocellulose fibers are partially dissolved and mobilized upon exposure to controlled amounts of an ionic liquid (IL) (1-ethyl-3-methyl imidazolium acetate (EMI-Ac) in our study), then reorganized upon IL removal [42]. Not only is NFW environmentally friendly and sustainable (ILs may be produced from biomass [43] and recycled), but the process often improves the mechanical properties of the welded fibers [42,44–47]. NFW can also be extended to the design of advanced functional materials, such as knittable energy storage textiles [48] and water treatment catalysts [40].

Using the methods reported in our pioneering study on lignocellulose-supported Pd–Cu catalysts [40], we first prepared a series of Pd–In catalysts, tailoring metal mass loadings to optimize catalytic performance towards nitrate reduction while preserving the underlying natural fiber support. While In has been shown to be an effective promotor metal in previous studies [23–27], catalyst composition, stability, and engineering performance for nitrate reduction of Pd–In bimetallics are still not well-understood. This is partially due to the very low amount of In (< 0.5 wt% with respect to the support) used in Pd–In catalysts, which challenges material characterization and mechanistic exploration. In the present study, we use a suite of characterization techniques to explore catalyst surface and bulk chemistry to understand relationships between catalyst properties, reactivity, and stability. In contrast to our Pd–Cu system previously reported, the Pd and In metals were more uniformly distributed throughout the natural fiber matrix due to the formation of a Pd–In alloy, and the resultant Pd–In catalysts were 10 times more reactive. Through nitrate reduction tests and X-ray photoelectron spectroscopy (XPS) depth profiling of aged Pd–In catalysts stored in air, we show that the Pd–In catalysts were also significantly more air-stable than Pd–Cu.

Next, the lignocellulose-supported Pd–In catalyst powders were immobilized onto extended lengths of linen yarn (as much as 79 m) using NFW methods that controlled the amount of catalyst welded to the yarn surface. These fiber-welded catalyst yarns were integrated into a uniquely engineered reactor optimized for nitrate reduction. Reactivity testing of the fiber-welded catalyst systems revealed a sustainable, reactive, robust catalytic structure, responsive to low-temperature H₂ regeneration at 105 °C, that remained stable during multiple reaction cycles in a myriad of real-world drinking water and wastewater matrices. This report represents a significant advance from our previous study. Not only do we present a new catalyst system that is 10 times more reactive, but we also present a full suite of material characterization data to show how and why the Pd–In catalyst remains stable during long-term storage. Through an exhaustive series of water tests, we reveal how to activate and regenerate this new catalyst system to achieve optimal performance for the catalytic reduction of nitrate from real-world complex waters. Furthermore, we present previously undisclosed NFW methods which demonstrate the scalability and control that can be exercised by this new, Green Engineering method in designing advanced functional materials for water purification.

2. Experimental section

2.1. Materials preparation

A full description of chemicals, materials, and methods is provided in the Supplementary Material. Each chemical or material was used as received. Yarns of linen (L) were milled to powder using a FlackTek Speed Mixer (DAC 150). Pd and Pd-In were loaded onto linen powder by incipient wetness (IW). The IW process involved impregnating powders with aqueous, metal nitrate solutions whose volume equaled the pore volume of the powder, the latter determined by the mass difference between dry and water-saturated fibers. Metal mass loadings were varied by adjusting the metal nitrate concentrations in solution. Following IW, the powders were air-dried, and then sequentially heated under N_2 and H_2 (120 °C for 2 h in each gas) to reduce the salts and produce metal nanoparticles. The following catalyst label code was used for catalyst powders: 'Substrate_wt%Pdwt%In'. Theoretical mass loadings of metals were reported in the code. For example, linen powder (L) with 5 wt% Pd and 1.2 wt% In was labeled L_5Pd1.2In.

For the NFW process, a known amount of the most reactive linen-supported Pd-In catalyst was suspended in a solution of EMI-Ac, acetonitrile and cotton (0.7 wt%). The resulting catalyst 'ink' was welded onto the surface of untreated linen yarn using a custom-built, proprietary yarn-coating system, first reported in a previous study [48], but modified with a syringe pump and control systems that enable control over catalyst loading. After yarns were coated with different amounts of catalyst, the IL was removed with water, and each sample was dried under N_2 at 60 °C. By this method, fiber-welded catalyst yarns were prepared with different catalyst mass loadings. One 15 m sample (containing ca. 0.2 mg of Pd-In catalyst metals per meter of yarn) was labeled 'NFW_Pd-In Low'. A second 15 m sample (containing ca. 0.4 mg of Pd-In catalyst metals per meter of yarn) was labeled 'NFW_Pd-In Med'. A final 79 m sample (containing 1.4 mg of Pd-In catalyst metals per meter of yarn) was divided into five 15 m sections (each labeled 'NFW_Pd-In High') for evaluation in five different water matrices.

2.2. Materials characterization

Full details of the materials characterization methods are provided in the Supplementary Material. Inductively coupled plasma-mass spectrometry (ICP-MS) (Agilent 7500) evaluated mass loadings of Pd and In; XPS (PHI 5600) identified the oxidation states of Pd, In, and C and surface concentrations of Pd, In, C, and O; attenuated total reflection-Fourier transform infrared spectroscopy (ATR-FTIR) (Nicolet iS10) probed the functional groups in the linen supports; scanning electron microscopy/energy dispersive X-ray spectroscopy (SEM/EDS) (TESCAN MIRA3, TEAM Octane SSD) examined the catalyst morphology, catalyst composition, and distribution of metals throughout the support and fiber-welded catalysts; and transmission electron microscopy (TEM) (Philips CM300 FEG) evaluated the metal nanoparticle morphology, composition, and crystal structure.

2.3. Powder catalyst nitrate reduction tests

To investigate catalyst performance towards contaminant removal, powdered catalysts were dispersed in ultrapure water with continuous H_2 and CO_2 bubbling. Prior to each test, the system was pre-sparged with H_2 for 30 min to activate metals that may have oxidized during storage in air [49]. During reduction tests, a H_2 flow of 150 $mL\ min^{-1}$ supplied sufficient reductant, and solutions were stirred at 500 rpm to eliminate mass transfer limitations [49]. An evaluation of mass transfer rates (see the Supplementary Material) indicated both aqueous/solid and intraparticle mass transfer did not influence the measured reactivities [40]. A CO_2 flow of 70 $mL\ min^{-1}$ maintained pH at ca. 4.5 during the reaction. During the reduction tests, nitrate concentrations were determined at regular time intervals by ion chromatography

(Dionex ICS-1100).

2.4. Powder catalyst stability tests

A series of experiments were performed to evaluate catalyst stability during storage in dry air. The catalyst with the highest In loading (L_5Pd2.6In) was selected to facilitate instrumental analysis. After synthesis, the catalyst was immediately divided into equal amounts and stored in a desiccator to control the air environment and ensure relative humidity below ca. 1%. At three intervals (day 0, 30, and 60), two samples were removed from the desiccator. One was immediately analyzed via XPS to investigate the degree the metals had oxidized during storage; the other was simultaneously evaluated for nitrate reduction kinetics. Following XPS analysis, the sample remained in the ultrahigh vacuum (UHV) chamber and was subjected to low energy argon ion (1 kV) sputtering at time intervals up to 180 min. In this manner, the degree of oxidation was determined for each 'aged' catalyst. A final nitrate reduction test was performed on a sample 'aged' in this way for 9 months.

2.5. NFW engineering of a catalyst reactor

Teflon jigs were manufactured with a CO₂ Hobby Laser (Full Spectrum) to hold 15 m samples of catalyst yarns during nitrate reduction tests. The chemical nature and the geometry of the jigs allowed each reactor assembly (i.e., fiber-welded catalyst yarn loaded onto the Teflon jig) to fit in the tube furnace and withstand the low temperature H_2 regeneration at 105 °C. Each 15 m section of fiber-welded Pd-In catalyst yarn was integrated onto a Teflon scaffold. A gas distribution system consisting of a manifold and four fused-silica diffusers was assembled, such that each diffuser fit into a quadrant of the Teflon jig. Upon integration, this distribution system mixed and evenly distributed H_2 and CO₂ to the catalyst yarns. Photographs of the reactor components are provided in the Supplementary Material (see Fig. S5).

2.6. Fiber-welded catalyst yarn nitrate reduction tests

The assembled reactors were fully submerged and tested in the following waters: (i) ultrapure water (18.2 MΩ·cm at 25 °C), (ii) finished drinking water from Frederick P. Griffith Jr. Water Treatment Plant ('GWP-Finished') using source water from the Occoquan Reservoir, VA, (iii) raw water from the Occoquan Reservoir, VA ('GWP-Raw'), (iv) finished water from Broad Run Water Reclamation Facility ('BRWRF-Finished'), and (v) effluent from BRWRF after membrane bioreactor (MBR) treatment ('BRWRF-Post MBR'). Water and wastewater treatment processes of GWP and BRWRF, and typical water quality parameters for each matrix, are reported in a previous study [50]. Before each series of water tests, the catalysts were regenerated by heat treatment under N_2 and H_2 at 105 °C (2 h in each gas). Test solutions were spiked with 0.1 mM nitrate, and nitrate concentrations were measured at regular intervals by ion chromatography (Dionex ICS-1100). Ammonia selectivity was determined by the Hach TNT 830 method via UV-vis spectrometry. Further experimental details are provided in the Supplementary Material.

3. Results

3.1. Structure and composition of lignocellulose-supported Pd-In catalysts

The linen-supported Pd-In catalyst powders were prepared by IW and a low-temperature hydrogen reduction method, as reported in our previous study [40]. SEM and EDS were used to evaluate the morphology and elemental distribution across the fiber matrix (Fig. 1). The SEM image (Fig. 1a) depicts a micron-sized catalyst fiber (L_5Pd1.2In) after it was milled into powder and loaded with nanoparticles containing Pd and In. The fiber morphology and diameter (ca. 10 m) are

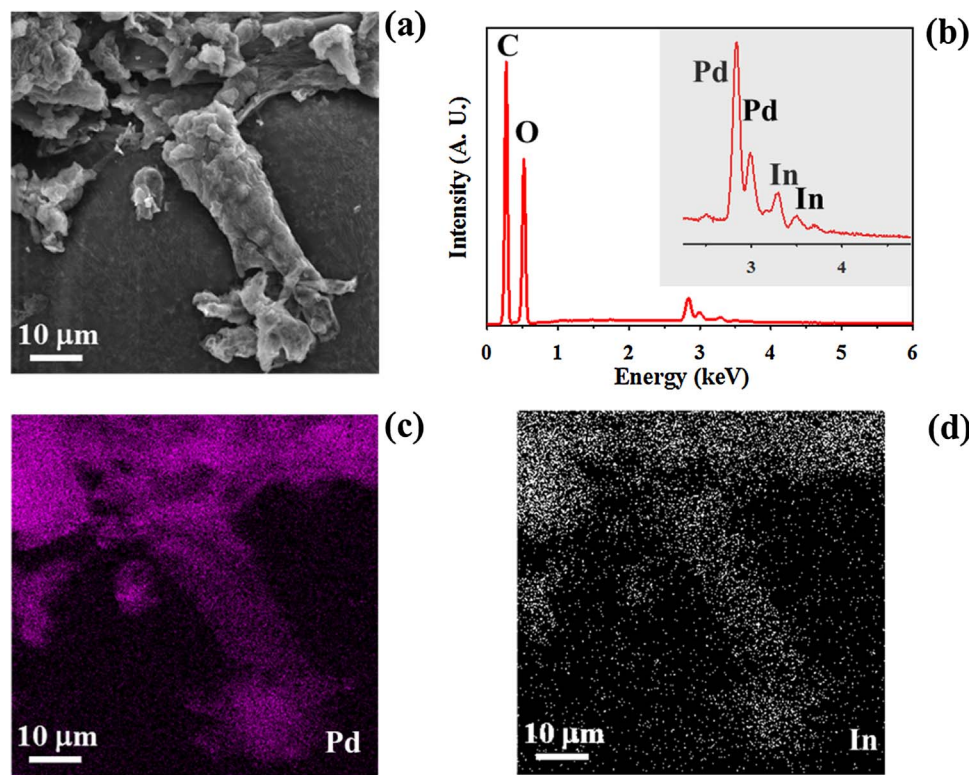


Fig. 1. Scanning electron microscopy (SEM) of a lignocellulose-supported Pd-In catalyst powder (L_5Pd1.2In). (a) An SEM image of the catalyst fibers (10 kV); (b) Energy dispersive X-ray spectroscopy (EDS) of a 16 mm^2 area of the catalyst fibers (20 kV); EDS elemental maps of the SEM image shows distribution of (c) Pd and (d) In on the catalyst fibers. Catalyst label code is: 'Substrate_wt%Pdwt%In', with "L" representing linen powder. The theoretical mass loadings of metals, represented by weight percentage, are reported in the code. In the EDS spectrum, intensity is presented in arbitrary units (A.U.).

similar to what was observed in the previous work [40]. EDS of a large (16 mm^2) region of the L_5Pd1.2In powder (Fig. 1b) determined that the fibers contained primarily C, O, Pd, and In, with an In/(In + Pd) of ca. 20 wt%. Elemental mapping of the fibers (Fig. 1c and d) clearly show that Pd and In were uniformly dispersed across the fiber matrix.

Bulk and surface elemental analyses for all powder catalysts was accomplished using ICP-MS, XPS, and EDS; these data are provided in the Supplementary Material (Fig. S1 and Table S1). The ICP-MS data are reported as weight percentage (wt%) of total catalyst, and compared with theoretical metal loadings determined from the mass of ions used in IW. Both XPS and EDS data are reported as atomic percentage (at%).

ICP-MS of nitric acid digested Pd-In catalyst powders revealed a close relationship between measured metal loading data and theoretical values, verifying that IW effectively loaded the correct composition of Pd and In onto the support. XPS measured the amount of Pd and In at the support surface (< ca. 10 nm); EDS semi-quantitatively assessed elemental composition at greater depths within the fiber matrix (ca. 750 nm to 9.5 μm, as determined by a Monte Carlo simulation [40,51]) by methods reported previously [40] and described in the Supplementary Material.

The XPS data on each Pd-In catalyst showed that Pd concentrations were 4–5 times higher than theoretical loadings, indicating that Pd preferentially deposited at the fiber surface, as was observed in our previous study of linen-supported Pd-based catalysts (Fig. S1a) [40]. The EDS data on each Pd-In catalyst showed that Pd compositions decreased exponentially ($R^2 = 0.88\text{--}0.92$) throughout the EDS-measured depths of the fiber (Fig. S1b). For each catalyst, the In concentrations were lower at the topmost surface layers (< ca. 10 nm, as measured by XPS), than in the near-surface regions measured by EDS, and like Pd, In concentrations also decreased exponentially ($R^2 = 0.90\text{--}0.94$) as acceleration voltage probed greater fiber depths (Fig. S1c). Combined, these XPS and EDS data show that, aside from having a Pd-rich surface, the In/(In + Pd) composition throughout the lignocellulose fibers was uniform (Fig. S1d). This was in contrast to linen-supported Pd-Cu catalysts [40], where different spatial distributions of Pd and Cu through

the fiber matrix resulted in a wide variation (30–40% difference) in Cu/(Cu + Pd) metal composition between the near-surface and bulk of the fibers [40].

3.2. Chemical characterization of metal nanoparticles

XPS was also used to characterize the catalyst bonding environment and oxidation state in the lignocellulose fibers. Fig. 2 shows the C(1s), Pd(3d), and In(3d) regions for representative Pd-In catalysts with a fixed Pd loading (5 wt%, theoretical) and various In loadings (0.9–2.1 wt%, theoretical). Irrespective of In loading, there was a Pd($3d_{5/2}/3d_{3/2}$) doublet in the Pd(3d) region consistent with the presence of a single species; the Pd($3d_{5/2}$) binding energy was located at 335.2 eV (± 0.1 eV), indicative of metallic Pd [52]. A slight shoulder, visible on the higher binding energy side of each Pd(3d) peak, may be attributed to some unreduced Pd^{2+} adsorbed on the surface.

Analysis of the In(3d) region indicated two peaks consistent with an In($3d_{3/2}/3d_{5/2}$) doublet, whose In $3d_{5/2}$ peak position suggests the presence of both In(0) (443.4 ± 0.1 eV) and In(III) (445.3 ± 0.1 eV) [52]. XPS depth profiling using high energy (4 kV) argon ions (data not shown) revealed that the catalysts were in fact zero valent indium with a thin layer of In(III), most likely In_2O_3 . XPS analysis of a control sample containing only In (L_1.2In, not shown) only showed peaks corresponding to In(III), confirming that Pd was required along with H_2 to effectively reduce the In^{3+} ions to the zero valent state.

Two primary carbon species were observed in the C(1s) region for every catalyst. The lower C(1s) binding energy region (284.5 eV) was attributed to alkyl carbon (i.e. $-\text{C}-\text{C}-$ or $-\text{C}-\text{H}$), and the higher binding energy region (> 286 eV) belonged to higher oxidation state carbon singly bonded to oxygen (i.e. the $\text{C}-\text{OH}$ and $-\text{C}-\text{O}-\text{C}$), both expected for lignocellulose supports [53]. Upon metal deposition, no significant shifts or new peaks were observed in the C(1s) envelope, indicating no chemical bonding interactions between the support and the metals. Infrared spectroscopy of the catalysts (provided in Fig. S2) also revealed no changes in spectra between untreated and treated fibers, confirming that the deposited Pd-In nanoparticles did not form chemical bonds

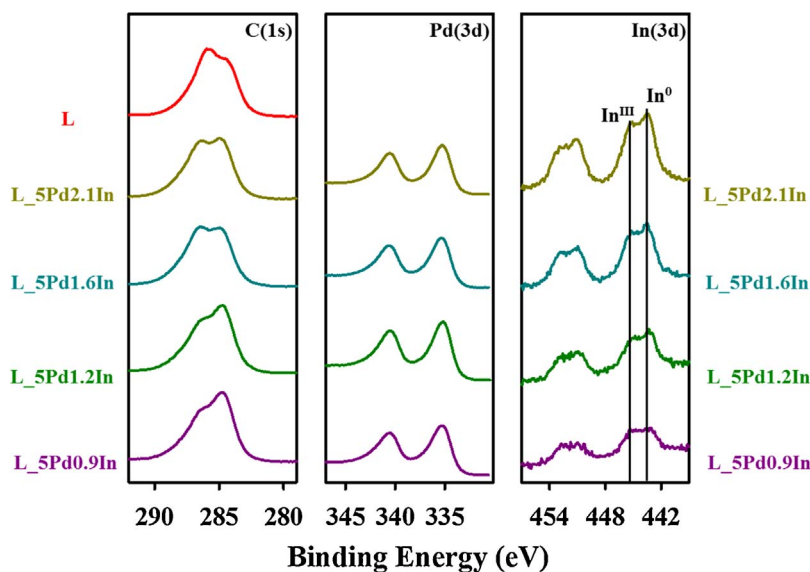


Fig. 2. X-ray photoelectron spectroscopy (XPS) of representative lignocellulose-supported Pd-In catalyst powders. Catalyst label code is: 'Substrate_wt%Pdwt%In', with 'L' representing linen powder. The theoretical mass loadings of metals, represented by weight percentage, are reported in the code.

with the polar oxygen-containing functional groups in the lignocellulose [40].

3.3. TEM characterization of the lignocellulose-supported Pd-In catalyst

The most reactive bimetal catalyst (L_5Pd1.2In) for nitrate reduction was analyzed with TEM to assess metal nanoparticle size, distribution, and structure (Fig. 3). One L_1.2In sample was also analyzed; however, the In-only sample did not form crystalline, zero valent In and only produced an amorphous selected area electron diffraction (SAED)

profile dominated by the lignocellulose substrate.

Low resolution TEM imaging (Fig. 3a) showed that the L_5Pd1.2In catalyst contained densely packed nanoparticles throughout the fibers. High-resolution TEM (HRTEM) images at the fiber edges (Fig. 3b) revealed near-spherical nanoparticles with sizes around 5–10 nm. All nanoparticles clearly showed lattice fringes, with little indication of the presence of amorphous material. The SAED pattern from an area ca. 5 μm in diameter acquired from the fiber edges of the catalyst is presented in Fig. 3c. The SAED profiles showed that each measured reflection (labeled A–E in Fig. 3c) was shifted to a lower $1/d$ value than

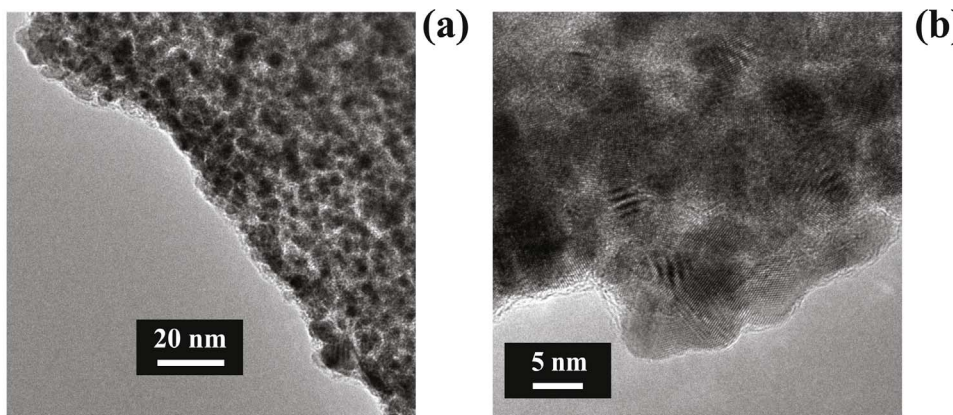
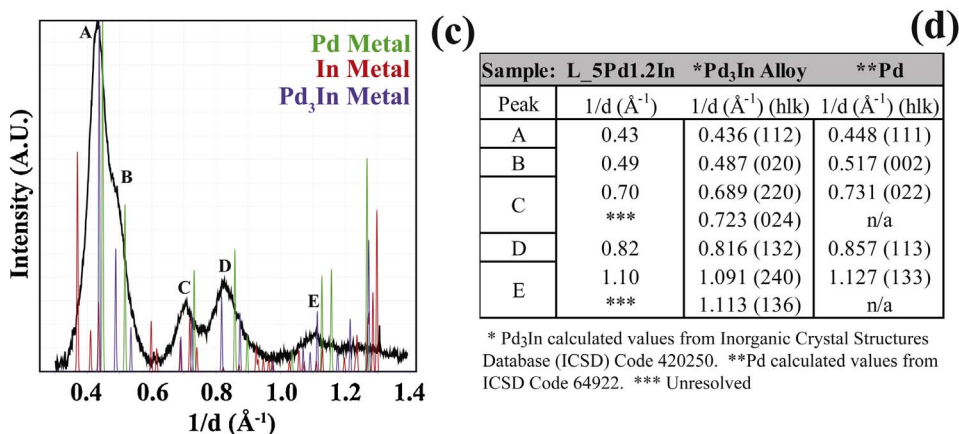


Fig. 3. Transmission electron microscopy (TEM) of a lignocellulose-supported Pd-In catalyst powder (L_5Pd1.2In). (a) A low resolution TEM image of the catalyst revealing densely packed Pd-In nanoparticles; (b) A high resolution TEM (HRTEM) image of the edge of the L_5Pd1.2In fibers; (c) A radially averaged selected area electron diffraction (SAED) profile of the nanoparticles indicates the presence of a Pd-In alloy; (d) The observed centroid peak positions for L_5Pd1.2In are compared to calculated reflections for Pd and Pd₃In as referenced in the Inorganic Crystal Structures Database (ICSD), with associated Miller Indices reported in parentheses. Catalyst label code is: 'Substrate_wt%Pdwt%In', with 'L' representing linen powder. The theoretical mass loadings of metals, represented by weight percentage, are reported in the code. In the SAED profile, intensity is presented in arbitrary units (A.U.).



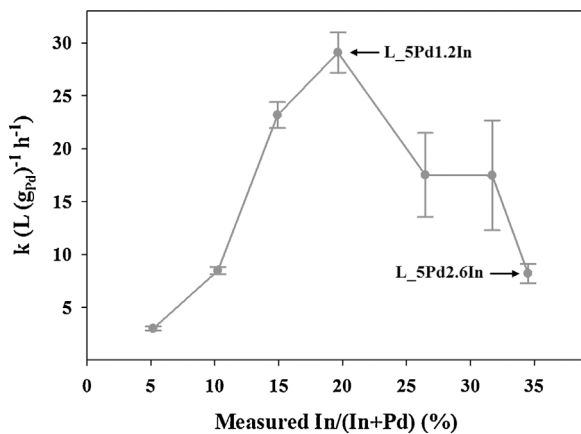


Fig. 4. Nitrate reduction rate constants of lignocellulose-supported Pd-In catalyst powders. The x-axis shows the catalysts measured In/(In + Pd) percentages as determined by ICP-MS (wt%). Pseudo-first-order rate constants are normalized to $\text{g}_{\text{Pd}} \text{ L}_{\text{rxnsoln}}^{-1}$ (i.e., Pd mass per volume of reaction solution) as determined by ICP-MS. Catalyst label code is: 'Substrate_wt%Pdwt%In', with "L" representing linen powder. The theoretical mass loadings of metals, represented by weight percentage, are reported in the code.

what would be expected for Pd metal, and toward SAED patterns indicative of Pd-In alloys. Fig. 3d compares the observed reflections for L_5Pd1.2In to the calculated reflections for pure Pd [54] and for the Pd₃In alloy [55].

These peak shifts are consistent with the phase being alloy, such as Pd₃In reported in the Inorganic Crystals Structures Database (ICSD), and are in agreement with previous studies showing that Pd and In readily form alloys [24,56,57]. However, the SAED patterns were not precise enough to determine the nanoparticles exact structure/composition.

EDS of the nanoparticles in the HRTEM image showed that both Pd and In were present (Fig. S3). The ratio of Pd to In measured in different nanoparticle regions appeared more uniform than what was observed in the Pd-Cu catalysts from our previous study, consistent with the XPS and EDS data that show Pd-In composition throughout the fibers was uniform.

3.4. Nitrate reduction of the Pd-In powder catalysts

Each Pd-In catalyst was assessed through nitrate reduction tests (Fig. 4) to determine the impact of In composition on catalytic

performance. The Pd-In catalysts were prepared with a theoretical Pd loading of 5 wt%, and varied theoretical In loadings from 0.3–2.6 wt%. Nitrate reduction rate constants were normalized to total mass of Pd metal (determined by ICP-MS) in the reaction solution (i.e., $\text{g}_{\text{Pd}} \text{ L}^{-1}$), and plotted as a function of each catalysts measured In/(In + Pd) percentage (wt%).

As In/(In + Pd) increased from 5 to 20%, nitrate reduction rate constants increased by an order of magnitude, from $3.0(\pm 0.2)$ to $29.1(\pm 1.9) \text{ L h}^{-1} \text{ g}_{\text{Pd}}^{-1}$. However, at higher In loadings, the nitrate reduction rate constants decreased steadily until reaching $8.2(\pm 0.9) \text{ L h}^{-1} \text{ g}_{\text{Pd}}^{-1}$ when the In/(In + Pd) percentage was 35%. Higher In loadings were not investigated. The most reactive L_5Pd1.2In catalyst (L_5Pd1.2In, $k = 29.1(\pm 1.9) \text{ L h}^{-1} \text{ g}_{\text{Pd}}^{-1}$) was 10 times more reactive than the most reactive L_Pd-Cu catalyst from a previous study tested under the same reaction conditions (L_5Pd3.3Cu, $k = 3.0(\pm 0.5) \text{ L h}^{-1} \text{ g}_{\text{Pd}}^{-1}$).

The Supplementary Material contains a performance comparison between our most reactive catalyst (L_5Pd1.2In) and Pd-In catalysts on other conventional supports (i.e., activated carbon, titanium dioxide, alumina, silica, and styrene divinylbenzene (Sty-DVB) resin) (see Table S2). Each Pd-In catalyst considered for this comparison was evaluated for nitrate reduction in batch reactors. Differences in reported results are expected due to the varied nature of each support and widely varied testing conditions (e.g., initial concentration of contaminant, catalyst loading, pH) used in each study.

3.5. Catalyst stability during storage in dry air

Nitrate reduction tests and XPS depth profiling were used to explore the stability of L_5Pd2.6In during nine months of storage in dry air; the results of this study are presented in Fig. 5. While no changes were seen in the C(1s) and Pd(3d) XPS spectra for each catalyst (data not shown), the amount of In(III), that represents In₂O₃, increased slightly from 37 to 56 at% (with respect to total In) from day 0–60 (Fig. 5a). Depth profiling of the samples 'aged' from day 0–60 consistently removed this thin oxide layer within 30 min of sputtering argon ions (Fig. 5b presents the XPS spectra after sputtering the 60-day old catalyst). In each sputtering experiment, as sputtering depth increased, the catalyst In/(In + Pd) concentration increased, ultimately approaching the EDS-measured metal ratios for an L_5Pd2.6In catalyst. This observation supports the conclusion reached by XPS and EDS that although the fiber surfaces were Pd-rich, just beneath the surface and into the bulk the Pd-In composition was more uniform.

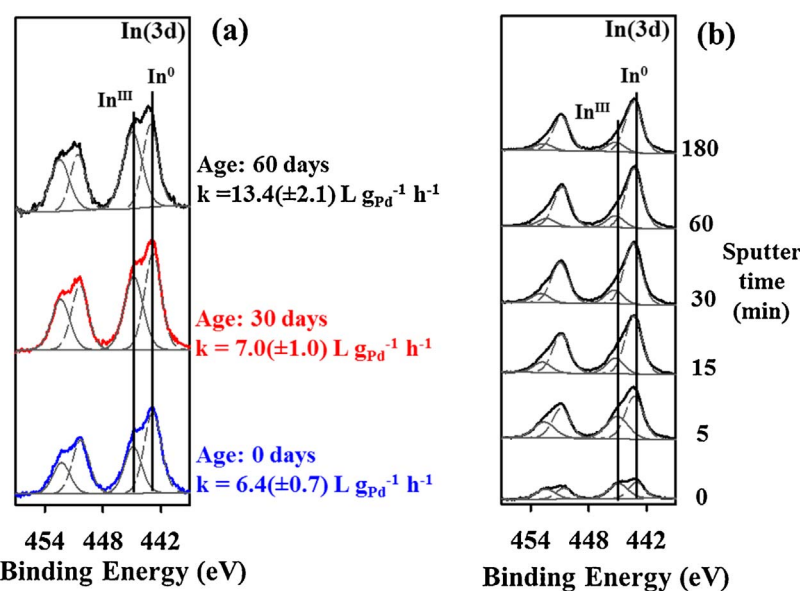


Fig. 5. Stability and reactivity of a lignocellulose-supported Pd-In catalyst powder (L_5Pd2.6In) stored in dry air. (a) X-ray photoelectron spectroscopy (XPS) of the catalyst, with catalyst age and corresponding nitrate reduction reactivity provided in the legend; (b) XPS of the 60-day old catalyst after argon ion sputtering (1 kV). Catalyst label code is: 'Substrate_wt%Pdwt%In', with "L" representing linen powder. The theoretical mass loadings of metals, represented by weight percentage, are reported in the code. Pseudo-first-order rate constants are normalized to $\text{g}_{\text{Pd}} \text{ L}_{\text{rxnsoln}}^{-1}$ (i.e., Pd mass per volume of reaction solution) as determined by ICP-MS.

Corresponding nitrate reduction tests of each aged sample (see Fig. 5a) revealed that the lignocellulose-supported Pd-In catalyst did not lose reactivity during extended storage in dry air. Between day 0 and 30, no significant change in reactivity was observed. After 60-days of storage, the catalysts observed rate constant was slightly higher, although within the same order of magnitude expected for its composition. After being stored for 9 months, a final nitrate reduction test revealed that the L₅Pd2.6In catalyst was still just as reactive ($k = 10.3(\pm 0.9) \text{ L h}^{-1} \text{ g}_{\text{Pd}}^{-1}$); because the reactivity did not significant change during 9 months of aging, further XPS analysis was not pursued. This lack of change in reactivity due to aging is consistent with the small changes seen by XPS for aged vs. as-prepared catalysts.

3.6. Scalable method to prepare catalyst yarns through natural fiber welding

Our previous work demonstrated NFW's potential to fabricate free-standing structures from lignocellulose-supported catalysts as a proof of concept [40]. In the current study, we present a new NFW method that can control catalyst loading onto a natural fiber substrate (linen yarn) through a simple, scalable process. Our goal was to design a welded-catalyst system to effectively reduce nitrate from complex water matrices that would be encountered in water and wastewater treatment environments.

Fig. 6 shows the general process used to fabricate and test the fiber-welded catalyst yarns, with a more complete description provided in the Supplementary Material. First, an IL-based 'ink' was prepared containing L₅Pd1.2In, the most reactive Pd-In powder catalyst. This 'ink' was delivered to the surface of untreated linen yarn at a desired rate, controlled by a syringe pump and/or the speed of the motor pulling the yarn. By using natural fiber welding (NFW), as much as 79 m of fiber-welded catalyst yarns were easily produced for a single experiment. While the powder catalysts for this work were developed with IW at the bench-scale, recent studies have presented IW as a scalable method to produce supported-nanoparticles. Zhang, et al. demonstrated scalable IW of Pt-based bimetal nanoparticles on carbon, alumina, silica, cesium oxide, and titanium oxide [58]. Kitamura, et al. studied a scalable method using sonication to support Pd nanoparticles on silk-fibroin [59]. Thus, in the current NFW application of welding catalyst to yarn, total process scalability will only be limited by the amount of catalyst and yarn available for the welding procedure; other reagents or solvents (e.g., EMI-Ac, acetonitrile) can be recycled.

SEM of each fiber-welded catalyst yarn (not shown) revealed how the NFW process delivered a thicker coating of to the linen yarn surface. ICP-MS was used to quantify the amount of metals actually welded onto each yarn (Table 1). Theoretical catalyst mass loadings on each fiber-welded yarn were approximated by the dry mass difference between treated/untreated samples and the theoretical IW loadings of the

L₅Pd1.2In powder. The measured bulk loadings in Table 1 represent an average of 5 yarn samples tested. The ICP-MS data revealed that some Pd and In was lost during the NFW reconstitution step, when water was used to remove IL from the yarn and stop the welding process. While some loss during reconstitution was not surprising, the data indicate that more In was lost than Pd in the rinse water, such that the final In/(In + Pd) composition (wt%) on the welded catalyst yarns was low (ca. 11–13%) compared to theoretical value of L₅Pd1.2In (20%). EDS measurements (not shown) of several regions of these coatings further confirmed an In/(In + Pd) composition (wt%) in the yarn coatings which varied between 9 and 14%. Aside from this metal loss, elemental mapping of the catalyst coating on 'NFW_Pd-In High' shows that the NFW process evenly distributed both Pd and In onto the yarn surface, while also welding the core of the yarn scaffold (Fig. S4), delivering a robust material that was easily integrated into a catalyst reactor (see Fig. 6 and Fig. S5) for nitrate reduction tests.

3.7. Nitrate reduction with fiber-Welded Pd-In catalysts

After being loaded onto the Teflon jig and integrated with the gas distribution system, each fiber-welded Pd-In catalyst was evaluated for nitrate reduction before and after low temperature H₂ regeneration at 105 °C in the tube furnace (Fig. 7). The regeneration process improved catalyst reactivity by ca. 31–58% after regeneration (compare tests (a) and (b) for each catalyst reported in Fig. 7). The reactivity of each regenerated fiber-welded catalyst system, normalized to catalyst loading (mass of Pd, as measured by ICP-MS) in the reaction solution were very similar to each other (within error). However, the nitrate reduction rate constants for the highest performing fiber-welded Pd-In catalyst was still ca. 3–4 times lower than the constituent powder catalyst of L₅Pd1.2In shown in Fig. 4. This reduction in performance was most likely due to the lower In/(In + Pd) (wt%) composition on the welded-yarns, due to preferential loss of In in the preparation which would decrease the In/Pd ratio and hence the reactivity of the alloy. Although gas-liquid mass transfer of H₂ may have decreased the fiber-welded catalyst performance, our control experiments showed how using the diffusers to increase catalyst exposure to H₂ improved the observed rate constant by more than 25%. While mass transfer limitations may also have been introduced by immobilizing the catalyst onto the support; the fact that the fiber-welded catalyst were only 3–4 times less reactive indicates this impact was minimal.

Next, five individual reactors each containing 15 m sections of yarn with the highest catalyst loading ('NFW_Pd-In High') were tested in increasingly complex water matrices. Each assembled reactor was immersed in a different water matrix, and the catalysts stability and effectiveness to reduce nitrate were evaluated. Fig. 8 shows these test results, normalized to catalyst loading (mass of Pd) in the reaction solution. ICP-MS of a test solution for dissolved Pd and In revealed that

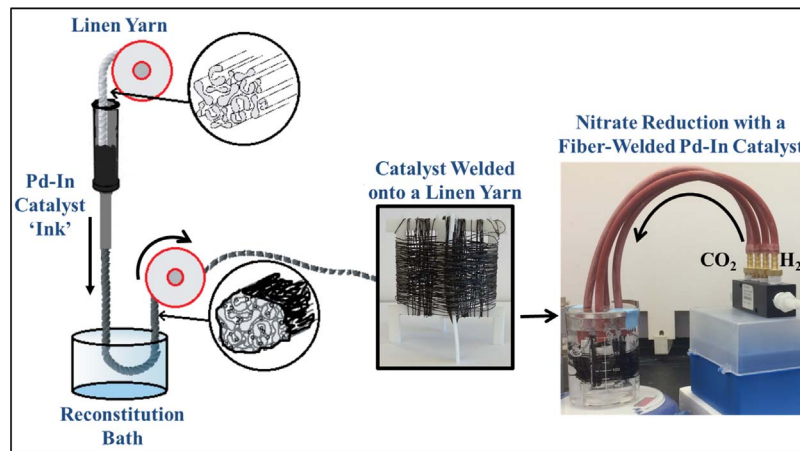


Fig. 6. Fabrication of a fiber-welded Pd-In catalyst yarn and its application for nitrate reduction.

Table 1Inductively coupled plasma-mass spectrometry (ICP-MS) of fiber-welded Pd-In catalyst yarns, with comparison to theoretical loadings.^a

Sample ID	Bulk Loading (ICP-MS)	Theoretical Loading (IW)	Bulk Loading (ICP-MS)	Theoretical Loading (IW)	Bulk Loading (ICP-MS)	Theoretical Loading (IW)	
Pd (wt%)			In (wt%)			In/(In + Pd) (wt%)	
NFW_Pd-In High	1.2 (0.2)	1.7	0.19 (0.1)	0.44	13.1 (2.9)	20.0	
NFW_Pd-In Med	0.4 (0.02)	0.7	0.05 (0.01)	0.19	11 (1.7)	20.0	
NFW_Pd-In Low	0.2 (0.1)	0.3	0.03 (0.01)	0.08	11.6 (2.2)	20.0	
L_5Pd1.2In (used for NFW)	5.1	4.9	1.2	1.2	19.0	20.0	
Reconstituted L_5Pd1.2In (IL-treated and water rinsed)	4.7	4.4	0.6	1.1	11.2	20.0	
Pd (ppm)			In (ppm)			In/(In + Pd) (wt%)	
Water used to rinse L_5Pd1.2In	3.2	–	1.2	–	28.3	–	

^a Bulk loading data are an average of 5 ICP-MS measurements, with standard deviation reported in parentheses. Theoretical loadings of Pd and In on the fiber-welded catalysts were estimated from IW theoretical values of the catalyst powder and the mass of the catalyst powder loaded on the yarns. Catalyst label code is: 'Substrate_wt%Pdwt%In', with 'L' representing linen powder. The theoretical mass loadings of metals on the powder, represented by weight percentage, are reported in the code. Fiber-welded catalyst yarns are labeled 'NFW_Pd-In Low/Med/High' and correlate with an increased catalyst metal loading.

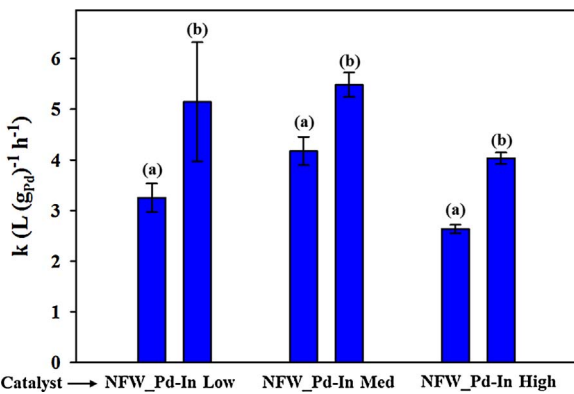


Fig. 7. Nitrate reduction performance for fiber-welded Pd-In catalyst yarns ('NFW_Pd-In Low/Med/High') (a) before catalyst regeneration and (b) after catalyst regeneration in the tube furnace under H₂ gas at 105 °C. Pseudo-first-order rate constants are normalized to g_{Pd} L_{rxnsoln}⁻¹ (i.e., Pd mass per volume of reaction solution) as determined by ICP-MS. Data for each 6 h nitrate reduction test are reported with error to 95% confidence intervals. Catalyst label code is: 'Substrate_wt%Pdwt%In', with 'L' representing linen powder. The theoretical mass loadings of metals, represented by weight percentage, are reported in the code. 'NFW_Pd-In Low/Med/High' correspond to loadings of 0.2/0.4/1.4 mg of Pd-In catalyst metals per meter of yarn.

negligible metals (< 0.001 wt% Pd and 0.01 wt% In, compared to the measured metals loaded on the yarn) leached into the reaction solution after more than 40 h of testing.

These results demonstrated the viability of using robust, stable and reactive lignocellulose-supported Pd-In catalyst systems to treat complex waters. However, differences were observed in measured rate constants for the 'NFW_Pd-In High' reactors tested in each water matrix (for example, compare 'test 3 in ultrapure water' to 'test 3 in GWP-Raw' shown in Fig. 8). Each fiber-welded Pd-In catalyst in the real water matrices appeared to exhibit slightly lower reactivity than the one tested in ultrapure water. A control experiment (described in the Supplementary Material) determined that higher background nitrate concentrations present in the GWP and BRWRF waters (see Table S3) were largely responsible for these lower observed rate constants. By accounting for these differences in initial nitrate concentrations, and comparing each catalyst's initial reaction rates instead of rate constants, it becomes more apparent that the fiber-welded catalyst's performance in ultrapure water, GWP-Raw, GWP-Finished, or BRWRF-Finished were quite similar (within error) (Fig. S6). The only catalyst that exhibited a slight reduction in initial reaction rate was the one tested in BRWRF-Post MBR; we believe that the presence of other constituents in BRWRF-Post MBR (i.e., alkalinity or organic matter) was the reason for this slight reduction in catalyst performance.

In each water matrix, the 'NFW_Pd-In High' catalyst reactivity increased slightly (14–40%) as the number of tests increased (see Fig. 8). We believe this effect was due to the catalysts prolonged exposure to the reducing environment at room temperature, (i.e., when the fiber-welded catalysts were exposed to water/H₂/CO₂ for ca. 18 h between tests 1–3). To test this hypothesis, a final experiment was performed. First, the 'NFW_Pd-In High' reactor (previously evaluated in ultrapure water) received a low temperature H₂ regeneration at 105 °C, and was conditioned in ultrapure water/H₂/CO₂ for 24 h prior to spiking nitrate and conducting any nitrate reduction tests. After this initial activation, the catalyst endured a single nitrate reduction test daily for 5 consecutive days. Between tests, the entire reactor assembly was stored in the water/H₂/CO₂ solution. Fig. 9 shows that, after the initial 24 h activation, a 43% improvement in reactivity was achieved in the first test, and the catalyst remained stable and highly reactive through 5 days (144 h) of testing. When the same experiment was conducted in GWP-Raw (using the 'NFW_Pd-In High' catalyst reactor previously evaluated in GWP-Raw), the initial 24 h activation improved the catalyst reactivity more than 60%. Differences in nitrate reduction rate constants between the 'NFW_Pd-In High' catalysts in each water matrix were due to higher initial nitrate concentration and natural organic matter in the GWP-Raw water.

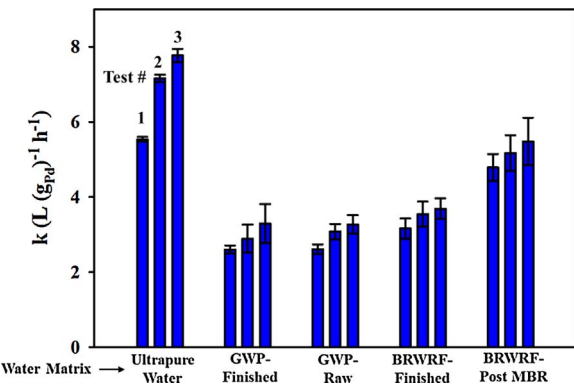


Fig. 8. Nitrate reduction performance of fiber-welded Pd-In catalyst yarn ('NFW_Pd-In High') in ultrapure water, as well as water matrices from the Frederick P. Griffith Jr. Water Treatment Plant (GWP) (using source water from the Occoquan Reservoir, VA) and the Broad Run Water Reclamation Facility (BRWRF). Pseudo-first-order rate constants are normalized to g_{Pd} L_{rxnsoln}⁻¹ (i.e., Pd mass per volume of reaction solution) as determined by ICP-MS. Data for each 6 h nitrate reduction test are reported with error to 95% confidence intervals. Each fiber-welded catalyst yarn contained 1.4 mg of Pd-In catalyst metals per meter of yarn.

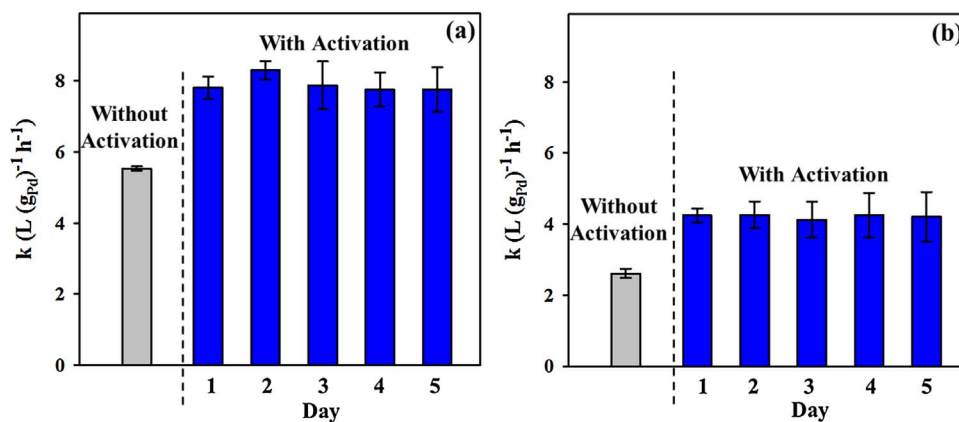


Fig. 9. Nitrate reduction performance for fiber-welded Pd-In catalyst yarn ('NFW_Pd-In High') before and after 24 h activation in ultrapure water with H_2/CO_2 bubbling. Following activation, testing occurred over 5 consecutive days of in the (a) ultrapure water matrix and in (b) raw water from the Frederick P. Griffith Jr. Water Treatment Plant (GWP-Raw). Each fiber-welded catalyst yarn was regenerated in the tube furnace under H_2 gas (105°C) prior to evaluation. Between each day of testing, the catalyst reactors were stored in ultrapure water with H_2/CO_2 bubbling for 18 h. Pseudo-first-order rate constants are normalized to $\text{g}_{\text{Pd}} \text{ L}_{\text{rxnsoln}}^{-1}$ (i.e., Pd mass per volume of reaction solution) as determined by ICP-MS. Data for each 6 h nitrate reduction test are reported with error to 95% confidence intervals. Each fiber-welded catalyst yarn contained 1.4 mg of Pd-In catalyst metals per meter of yarn.

4. Discussion

4.1. Lignocellulose supported Pd-In nanoparticle catalysts

In our previous study, we demonstrated how lignocellulose fibers from linen and bamboo yarns could be used as sustainable supports to grow small (5–10 nm) Pd and Pd-Cu nanoparticles while maintaining the integrity of the natural fiber support [40]. That study revealed that the nanoparticles were not chemically bonded to the support and that the catalyst fibers could be post-processed through NFW without negatively impacting catalyst performance. In the present study, we used the same IW method and low temperature thermal treatment in N_2 and H_2 to prepare a series of Pd-In nanoparticle catalysts on linen fibers. Material characterization of the linen powder supported catalysts was largely in agreement with results from our previous study, principally (i) Pd-In nanoparticle catalysts were not chemically bonded to the supports, (ii) Pd preferentially reduced at the fiber surface, (iii) Pd-In nanoparticles were small (ca. 5–10 nm) metallic and crystalline, with Pd-In alloys at the fiber edges, and (iv) the integrity of the support was maintained throughout the metal deposition process, allowing it to be post-processed via NFW.

Despite the marked similarities, we uncovered three distinct differences between Pd-Cu and Pd-In nanoparticles on lignocellulose fibers. Compared to Pd-Cu, the Pd-In catalyst had a more uniform composition, was up to 10 times more reactive when tested under the same reaction conditions, and exhibited extremely high stability during storage in air. The following discussion suggests how these three observations are inter-related.

The EDS analysis of each catalyst revealed the Pd-In metals were more uniformly distributed throughout the lignocellulose fibers as compared to the Pd-Cu system (see Fig. S1). This observation was supported by data acquired from TEM and XPS depth profiling of the Pd-In powder catalysts. We conclude that a more uniform Pd-In distribution on lignocellulose enhanced the catalytic activity, allowing more nitrate ions to interact with and be reduced by catalyst of the optimal composition. Many reports, including the present study, have shown how a catalyst's performance is influenced by promotor/noble metal composition on various supports [19,24,27,56,60–62]. It is possible that the observed Pd-In uniformity was a result of Pd-In alloy formation, which was detected in the TEM analysis of the L_5Pd1.2In catalyst (see Fig. 3). Previous studies have established that Pd and In will easily form alloys under reducing environments at or slightly above room temperatures [24,25,57,60]. In the synthesis of Pd-In on lignocellulose, the metals' exposure to H_2 at 120°C likely allowed Pd-In to mix together as each reduced to their zero-valent state (as measured by XPS) and formed the air-stable alloy.

A thin oxide layer on the In metal (observed in XPS and removed by ion sputtering) also likely contributed to the catalysts high air-stability. The Pd-In nanoparticles prepared in this study were crystalline

(determined by TEM), and contained primarily zero valent Pd and zero valent In (determined by XPS). In the presence of O_2 , crystalline In metal will quickly develop a thin, conductive oxide layer that can protect it from further oxidation [63]. With the crystalline Pd-In nanoparticles in our study, this In_2O_3 layer formed immediately upon exposure to the atmosphere, and had limited growth (< 19% as determined by XPS of aged samples) during 2 months of storage in the desiccator (see Fig. 5). Any oxidation that did occur on the Pd-In nanoparticles during storage could easily be remediated with the low temperature thermal treatment in H_2 gas at 105°C . We hypothesize this thin oxide layer did not degrade catalyst reactivity because In_2O_3 thin films are conductive [64,65], with reported resistivities in the range of $1 \times 10^{-6} \Omega\text{m}$ [66]. Although this is not as conductive as Indium metal (resistivity ca. $8 \times 10^{-8} \Omega\text{m}$) [67], the thinly oxidized promotor metal nanoparticles were still conductive enough to allow any electron transfer and oxygen atom transfer processes to occur during nitrate reduction. Using XPS in a previous study, Chaplin, et al. also detected a surface layer of In_2O_3 on alumina-supported Pd-In catalysts, postulating that underlying zero valent In (also detected with XPS) still played a vital role for nitrate reduction despite the surface In_2O_3 layer [68].

4.2. Nitrate reduction reactivity and stability with Pd-In lignocellulose powder catalysts

The lignocellulose-supported Pd-In catalysts exhibited an optimum composition for enhanced reactivity towards the catalytic hydrogenation of nitrate (see Fig. 4). Previous studies have reported optimal In/(In + Pd) (wt%) for nitrate reduction on other supports, including silica (20%) [56], alumina (17–29%) [19,24,56], activated carbon (20%) [60], titanium dioxide (29%) [62], and sty-DVB resin (20%) [27]. Pd-In composition has also been optimized on alumina for N-nitrosodimethylamine reduction (20%) [23]. Our results are comparable to these previous studies, with the most reactive Pd-In catalyst having an optimum In/(In + Pd) percentage of 20%. The existence of an optimum In loading indicates that In is an important promotor metal for nitrate reduction, and that Pd-In interactions critically enhance the rate of reaction as shown in previous studies [19,24,27,56,61]. These studies show sufficient In sites, in direct contact with or in close proximity to Pd, are needed to promote catalytic nitrate reduction. However, excessive amounts of In likely reduce the number of accessible Pd surface sites, limiting the hydrogen dissociation required to regenerate zero valent In for nitrate reduction and the reduction of other reaction intermediates (e.g., NO_2^- , N_2O) on Pd.

When comparing L_5Pd1.2In to similar Pd-In catalysts loaded on conventional supports, it is clear that our catalyst has comparable performance for nitrate reduction (see Table S2). Many studies have shown that reaction pH, reagent concentrations, and support characteristics all impact the nitrate reduction rates of Pd-In catalysts [11,19,25,27,60]. Prusse, et al. also showed how the availability of Pd

active sites in Pd-based bimetal catalysts can also control selectivity of nitrate reduction to either nitrogen gas or ammonia [19]. Krawczyk, et al., showed how increased amounts of the Pd-In alloy, supported on titanium dioxide, will drive the nitrate selectivity toward ammonia [62]. In the present study, the lignocellulose-supported Pd-In catalysts had relatively high selectivity toward ammonia (63–76% compared to initial nitrate concentration) when reduction was complete and the nitrate concentration was below the detection limit (Table S3). While this result is undesirable for water purification, and may be in part to the presence of Pd-In alloy nanoparticles, many studies have shown that ammonia selectivity can also be governed by other parameters (i.e., initial nitrate concentrations, H₂ supply, pH, and water quality) [24,28,49,69,70], which should be explored and optimized in future studies.

4.3. Sustainable and scalable engineering of a lignocellulose-supported Pd-In catalyst

Emergent water treatment catalysts are often first tested in batch reactors [23–26,71], to optimize catalyst development and understand the impact of water chemistry for catalytic performance, before they are integrated into more advanced applications. Fine powder catalysts are typically used for these batch reactions, while pelletized catalysts (e.g., supported on porous alumina or activated carbon) with a larger particle size are used in flow-through reactors, such as catalyst-packed beds [16,17,69,72], to treat contaminants in a continuous mode. However, these powder and pelletized catalysts are difficult to recover, regenerate, or reuse. Although our fiber-welded catalysts were evaluated in a semi-batch reactor, in their present form they are also well-suited for incorporation into continuous-flow reactors. Not only do lignocellulose-supported Pd-In catalysts exhibit comparable reactivity, but they are easily recovered for subsequent regeneration/reuse compared to powders or pellets.

Typically, embedding reactive metals (e.g., Pd, and other promoters) into the porous structure of conventional catalyst supports for these continuous-mode applications slows mass transfer rates of reactants, significantly limiting their catalytic reactivity. For example, when Pintar, et al. presented the first integrated ion-exchange/hydrogenation catalyst hybrid, an alumina-supported Pd–Cu packed-bed reactor [33], they observed extremely low reactivity (compared to the same catalyst powder tested in a batch reactor [21]). They attributed their results to poor gas-liquid mass transfer of H₂. Due to this mass transfer limitation, Pintar, et al. concluded that only ca. 1–10% of the catalyst was being exploited to reduce nitrate in the fixed-bed configuration. More recently, Bergquist, et al. observed 25 times lower reactivity in their Pd-In catalyst on activated carbon, when tested in a similar packed-bed reactor, as compared to the same powder tested in a batch reactor [17], also attributing the loss to limitations of mass transport of H₂ to the immobilized catalyst. In contrast, the reactivity of our fiber-welded Pd-In catalyst reactor was only 3–4 times less reactive than its constituent L₅Pd1.2In powder.

It is plausible that the fiber-welded Pd-In catalyst retained more of its catalytic reactivity (as compared to previous studies using conventional supports [17,33]) due to the porous, hydrophilic nature of the linen fibers. These physical characteristics may have lessened potential impacts from reduced aqueous/solid mass transfer rates of nitrate to the catalyst surface. Some of the observed loss in reactivity may still be due to poor gas-liquid mass transport of H₂, as was suggested by both Pintar, et al. [33] and Bergquist, et al. [17]. The fact that the fiber-welded catalysts performance improved 25% after gas diffusers were integrated into the reactor supports this hypothesis, although the current testing configuration makes a quantitative assessment of mass transfer impacts challenging. We conclude that the primary reason the fiber-welded catalyst were less reactive was due to metal loss that occurred during NFW reconstitution, when IL was rinsed from the yarns to quench the welding process. Regardless, the performance of the present

system is significantly improved compared to previous continuous-mode reactor designs.

Some physical loss of both metals during the NFW reconstitution was expected, as the nanoparticles were not covalently bound to the lignocellulose support. However, it is unclear chemically why more In than Pd was lost when water was used to rinse out the IL. As a noble metal, Pd should not be oxidized in water, and despite its lower standard redox potential, neither should In (In³⁺/In –0.338 V vs. NHE; Pd²⁺/Pd 0.915 V vs. NHE) [73]. Nor should Pd or In be impacted by acetonitrile (the co-solvent in the NFW ‘ink’), a common solvent used for sol-gel synthesis of metal nanoparticles such as In [74]. In metal is known to be susceptible to oxidation in acidic media (i.e., the mineral acids [75,76] as well as acetic acid [77]), but the imidazolium cation has extremely low acidity and is not likely to oxidize either metal [78]. Any acidic character in EMI-Ac would come from the slight excess of acetic acid used in the synthesis of EMI-Ac to mitigate IL decomposition to carbene [79,80]. Because the acid content of EMI-Ac is typically very low (less than 1 wt% as measured by titration in the present study) [44], it is very unlikely the NFW ‘ink’ solution or rinsing agent were the cause of this metal loss; however, we have insufficient data at this time to rule out either possibility. We remain confident that this challenge will be overcome with further optimization of the NFW process, and that the full potential of fiber-welded Pd-In catalysts can be realized. Once assembled, however, the fiber-welded Pd-In catalysts did not leach metal (Pd or In) during prolonged exposure to the slightly acidic (pH 4.5) environment of the nitrate reduction tests, a pH lower than anything expected in the NFW ‘ink’, and their reactivity remained high and stable during more than 180 h of evaluation over 4 months. This is consistent with the sustained level of reactivity observed over time as shown in Fig. 9.

The NFW process proved to be an effective way to deliver a controlled amount of catalyst to the surface of the linen yarn support. By changing the syringe pump rate during the welding process, different amounts of L₅Pd1.2In were delivered to the yarn (Table 1), and nitrate reduction tests of each system (Fig. 7) showed how catalyst loading impacted nitrate reduction performance. The catalytic reactivity of each NFW_Pd-In catalyst (i.e., Low, Med, and High) was very close, indicating a similar degree of catalyst active sites were accessed with each reactor and that mass transport was not significantly limiting catalyst performance.

Although the catalysts observed rate constants were lower in the complex waters, this was due to primarily to higher initial nitrate concentrations (see the Supplementary Material). Lemaignen, et al. reported a similar initial nitrate concentration effect during a study of Pd-In catalysts supported on activated carbon [60]. To a lesser degree, catalyst performance was slightly degraded by other constituents present in the water, such as alkalinity and/or (natural) organic matter. In a previous study, Chaplin, et al. demonstrated that these constituents can inhibit Pd-based catalysts during nitrate reduction [81]. Interestingly, during each testing sequence, our Pd-In catalysts performance always increased from test 1 to test 3, indicating some benefit from extended exposure to the reducing environment. We ascribe this effect to the catalyst activation that occurred during continuous exposure to the reducing environment in the test solution. Our final evaluation (shown in Fig. 9) showed that this 24 h activation period in H₂ and CO₂, in the absence of nitrate, should be used to condition the fiber-welded Pd-In catalysts for optimal performance.

4.4. Environmental implications

In combination, lignocellulose-supported Pd-based catalysts and the NFW method are an environmentally friendly alternative to water treatment solutions using conventional catalyst supports. The catalysts are prepared through IW, which can be engineered in a scalable manner. The remarkable stability of the lignocellulose-supported Pd-In catalyst, combined with the negligible amount of metals that leached

from the welded yarns, are a testament to the sustainable, robust nature of the product NFW delivers. Not only can NFW strongly adhere the catalyst fibers to the linen yarn support, but the process can be controlled to deliver different catalyst loadings, and its scalability is only determined by the amount of catalyst and yarn used during the welding process. With the current methods and technology highlighted in this study, for example, one mile of 'NFW_Pd-In High' could easily be prepared in our lab today and would consume only ca. 9 g of Pd and 2.3 g of In; this would be enough catalyst to assemble a portable, stand-alone system with a 100-fold increase in capacity. Because our catalysts show high reactivity and are not significantly mass-transport limited, they are viable candidates for membrane reactors [82], trickle-beds [33], hybrid flow-through systems [17], or alternative free-standing, portable fiber-welded designs. However, mass transfer between the gas/liquid/solid interfaces must continue to be critically evaluated in future applications to realize the full potential of NFW catalyst systems for water treatment. Additionally, fiber-welded catalysts are easy to separate from the test solution, exchange for fresh catalyst, and regenerate for subsequent use. While our study shows how a low temperature thermal treatment in H₂ effectively regenerates Pd-In catalysts by reducing oxidized metals, other chemical methods (i.e., treatment with hypochlorite, as shown by Chaplin, et al.) [68] can also be applied to restore Pd-In catalyst performance after it has been fouled, for example by reduced sulfur species in complex waters.

It is clearly an advantage that lignocellulose-supported catalysts can be post-processed via NFW, at scale and sustainably using environmentally friendly ILs (which can be recycled). To advance the technology beyond this study, some NFW processing steps must be further optimized (for example, determining how to remove IL with little or no impact to catalyst metal composition). Regardless, NFW offers a cost-effective, sustainable, eco-friendly alternative for engineering catalysts in real-world water treatment. Beyond this application, our study shows the promise that NFW holds as a platform for introducing functional-cellulose systems into other technologies, for example as photocatalysts, sustainable ion-exchange systems, energy storage technologies, bioremediation, sensing, and multi-functional reinforcement materials for synthetic polymers.

5. Conclusion

This report showed that lignocellulose-supported palladium-indium (Pd-In) catalysts were 10 times more reactive and more air-stable than Pd-Cu catalysts prepared in a similar method from our previous study. The catalyst powders contained small (5–10 nm), near-spherical Pd-In nanoparticles loaded on milled linen fibers, with Pd-In alloy and a uniform Pd-In metal composition throughout the support. Through *Natural Fiber Welding* (NFW), the lignocellulose-supported Pd-In powders were welded onto untreated linen yarn, using a custom-built yarn-coating system and a scalable process that controlled catalyst loading onto the support. The welded Pd-In catalyst yarns were integrated into a novel water treatment system, and procedures were optimized to maximize the reaction rate constants for nitrate reduction, including (i) catalyst regeneration in low temperature thermal treatment in H₂ at 105 °C (leading to a 31–58% increase of reactivity), (ii) enhanced H₂ distribution to catalyst via gas diffusers (leading to a 25% increase of reactivity), and (iii) 24-h activation period exposing the catalyst to an aqueous reducing environment (leading to a 43–60% increase of reactivity). Through more than 180 h of evaluation during a four-month period of nitrate reduction tests in ultrapure water, the fiber-welded Pd-In catalyst reactor remained reactive and stable, showing no signs of degradation and no detectable metal leaching. When tested in raw or (partially) treated water and wastewater, the fiber-welded catalysts were also reactive and robust, with minimal adverse impact due to naturally occurring constituents in the complex water matrices. Our study highlights a scalable approach through NFW to design water treatment system components using green engineering methods and

sustainable catalyst support materials. The evaluation of fiber-welded catalyst reactors represents a significant advance towards designing a commercially relevant system to meet the challenges of nitrate decontamination in complex, real-world water matrices. Beyond water treatment, the highlighted methods offer a sustainable platform for using functional-cellulose systems in a wide-array of technologies, including photocatalysis, energy storage, sensing, and bioremediation.

Conflicts of interest

The authors declare no competing financial interest. Any opinions, findings and conclusions, or recommendations expressed in this manuscript are those of the authors and do not reflect the views of the U.S. Air Force or the U.S. Navy.

Acknowledgements

We acknowledge the National Science Foundation (NSF) grant CBET-1437989, startup funds from the Department of Civil and Environmental Engineering, The George Washington University (GW), and the Johns Hopkins University Water SEED grant for supporting our study. We are grateful to the Air Force Office of Scientific Research for funding, and Johns Hopkins University and the U.S. Naval Academy for facilities support. We also thank John J. Hanchak at GWP and Michael R. Rumke at BRWRF for providing water samples.

Appendix A. Supplementary data

Supplementary data associated with this article can be found, in the online version, at <http://dx.doi.org/10.1016/j.apcatb.2017.09.029>.

References

- [1] K.R. Burow, B.T. Nolan, M.G. Rupert, N.M. Dubrovsky, *Environ. Sci. Technol.* 44 (2010) 4988–4997.
- [2] R.F. Spalding, M.E. Exner, *J. Environ. Qual.* 22 (1993) 392–402.
- [3] F.T. Wakida, D.N. Lerner, *Water Res.* 39 (2005) 3–16.
- [4] J.R. Degnan, J.K. Bohlike, K. Pelham, D.M. Langlais, G.J. Walsh, *Environ. Sci. Technol.* 50 (2015) 593–603.
- [5] L. Fewtrell, *Environ. Health Perspect.* 112 (2004) 1371–1374.
- [6] S.S. Mirvish, *Nat. Mater.* 315 (1985) 461–462.
- [7] P.J. Weyer, J.R. Cerhan, B.C. Kross, G.R. Halberg, J. Kantamneni, G. Breuer, M.P. Jones, W. Zheng, C.F. Lynch, *Epidemiology* 11 (2001) 327–338.
- [8] WHO, *Guidelines for Drinking-water Quality*, World Health Organization, Geneva, 2008.
- [9] USEPA, *National Primary Drinking Water Regulations*, In: USEPA (Ed.), US Government Printing Office, Washington DC, 2010.
- [10] A. Kapoor, T. Viraghavan, *J. Environ. Eng.* 123 (1997) 371–380.
- [11] U. Prusse, M. Hahnlein, J. Daum, K.D. Vorlop, *Catal. Today* 55 (2000) 79–90.
- [12] Y. Yoshihaga, T. Akita, I. Mikami, T. Okuhara, *J. Catal.* 207 (2001) 37–45.
- [13] O.M. Ilinitch, L.V. Nosova, V.V. Gorodetskii, V.P. Ivanov, S.N. Trukhan, E.N. Gribov, S.V. Bogdanov, F.P. Cuperus, *J. Mol. Catal. A: Chem.* 158 (2000) 237–249.
- [14] S. Horold, K.D. Vorlop, T. Tacke, M. Sell, *Catal. Today* 17 (1993) 21–30.
- [15] M.G. Davie, H. Cheng, G.D. Hopkins, C.A. LeBrun, M. Reinhard, *Environ. Sci. Technol.* 42 (2008) 8908–8915.
- [16] J.K. Choe, A.M. Bergquist, S. Jeong, J.S. Guest, C.J. Werth, T.J. Strathmann, *Water Res.* 80 (2015) 267–280.
- [17] A.M. Bergquist, J.K. Choe, T.J. Strathmann, C.J. Werth, *Water Res.* 96 (2016) 177–187.
- [18] J.K. Choe, M.H. Mehnert, J.S. Guest, T.J. Strathmann, C.J. Werth, *Environ. Sci. Technol.* 47 (2013) 4644–4652.
- [19] U. Prusse, K. Vorlop, *J. Mol. Catal. A: Chem.* 173 (2001) 313–328.
- [20] F. Gauthard, F. Epron, J. Barbier, *J. Catal.* 220 (2003) 182–191.
- [21] A. Pintar, J. Batista, J. Levec, T. Kajiiuchi, *Appl. Catal. B* 11 (1996) 81–98.
- [22] A. Pintar, G. Bercic, J. Levec, *AIChE J.* 44 (1998) 2280–2292.
- [23] M.G. Davie, K. Shih, F.A. Pacheco, J.O. Leckie, M. Reinhard, *Environ. Sci. Technol.* 42 (2008) 3040–3046.
- [24] I. Witońska, S. Karski, J. Rogowski, N. Krawczyk, *J. Mol. Catal. A: Chem.* 287 (2008) 87–94.
- [25] F.A. Marchesini, S. Irusta, C. Querini, E. Miró, *Catal. Commun.* 9 (2008) 1021–1026.
- [26] R. Zhang, D. Shuai, K.A. Guy, J.R. Shapley, T.J. Strathmann, C.J. Werth, *ChemCatChem* 5 (2013) 313–321.
- [27] D.P. Barbosa, P. Tchiéta, M.C. Rangel, F. Epron, *J. Mol. Catal. A: Chem.* 366 (2013)

294–302.

[28] J. Batista, A. Pintar, M. Ceh, *Catal. Lett.* 43 (1997) 79–84.

[29] K. Wada, T. Hirata, S. Hosokawa, S. Iwamoto, M. Inoue, *Catal. Today* 185 (2012) 81–87.

[30] S. Verma, M. Nandi, A. Modak, S.L. Jain, A. Bhaumik, *Adv. Synth. Catal.* 353 (2011) 1897–1902.

[31] M. Kim, S. Chung, C. Yoo, M. Lee, I. Cho, D. Lee, K. Lee, *Appl. Catal. B* 142–143 (2013) 354–361.

[32] O. Soares, J. Orfao, M. Pereira, *Appl. Catal. B* 91 (2009) 441–448.

[33] A. Pintar, J. Batista, *Catal. Today* 53 (1999) 35–50.

[34] P. Bayer, E. Heuer, U. Karl, M. Finkel, *Water Res.* 39 (2005) 1719–1728.

[35] K. Hjaila, R. Baccar, M. Sarra, C.M. Gasol, P. Blanquex, *J. Environ. Manage.* 130 (2013) 242–247.

[36] F. Quignard, A. Choplin, *Chem. Commun.* 2000 (2001) 21–22.

[37] J. He, T. Kunitake, A. Nakao, *Chem. Mater.* 15 (2003) 4401–4406.

[38] K. Reddy, N. Kumar, P. Reddy, B. Sreedhar, M. Kantam, *J. Mol. Catal. A: Chem.* 252 (2006) 12–16.

[39] S. Padalkar, J. Capadona, S. Rowan, C. Weder, Y. Won, L. Stanciu, R. Moon, *Langmuir* 26 (2010) 8497–8502.

[40] D.P. Durkin, T. Ye, E.G. Larson, L.M. Haverhals, K.J.T. Livi, H.C. De Long, P.C. Trulove, D.H. Fairbrother, D. Shuai, *ACS Sustain. Chem. Eng.* 4 (2016) 5511–5522.

[41] L.M. Haverhals, W.M. Reichert, H.C. De Long, P.C. Trulove, *Macromol. Mater. Eng.* 295 (2010) 425–430.

[42] L.M. Haverhals, L.M. Nevin, M.P. Foley, E.K. Brown, H.C. De Long, P.C. Trulove, *Chem. Commun.* 48 (2012) 6417–6419.

[43] J. Hulbosch, D.E. De Vos, K. Binnemans, R. Ameloot, *ACS Sustain. Chem. Eng.* (2016) Article ASAP.

[44] L.M. Haverhals, H.M. Sulpizio, Z.A. Fayos, M.A. Trulove, W.M. Reichert, M.P. Foley, H.C. De Long, P.C. Trulove, *Cellulose* 19 (2012) 13–22.

[45] L.M. Haverhals, H.M. Sulpizio, Z.A. Fayos, M.A. Trulove, W.M. Reichert, M.P. Foley, H.C. De Long, P.C. Trulove, *Electrochem. Soc. Trans.* 33 (2010) 79–90.

[46] L.M. Haverhals, T.A. Isaacs, E.C. Page, W.M. Reichert, H.C. De Long, P.C. Trulove, *Electrochem. Soc. Trans.* 16 (2009) 129–139.

[47] L.M. Haverhals, H.M. Sulpizio, Z.A. Fayos, M.A. Trulove, W.M. Reichert, M.P. Foley, H.C. De Long, P.C. Trulove, *Electrochem. Soc. Trans.* 33 (2010) 91–98.

[48] K. Jost, D.P. Durkin, L.M. Haverhals, E.K. Brown, M. Langenstein, H.C. De Long, P.C. Trulove, Y. Gogotsi, G. Dion, *Adv. Funct. Mater.* 5 (2014) 1–8.

[49] D. Shuai, J.K. Choe, J.R. Shapley, C.J. Werth, *Environ. Sci. Technol.* 46 (2012) 2847–2855.

[50] Q. Zheng, D.P. Durkin, J.E. Elenewski, Y. Sun, N. Banek, L. Hua, H. Chen, M.J. Wagner, W. Zhang, D. Shuai, *Environ. Sci. Technol.* 50 (2016) 12938–12948.

[51] J. Bausells, *Electron Interaction with Solids – Single Scattering Monte Carlo Simulation Software*, Barcelona, Spain 2008, Pp. *Electron Interaction with Solids – Single Scattering Monte Carlo Simulation Software*, (2008).

[52] J.F. Moulder, W.F. Stickle, P.E. Sobol, K.D. Bomben, *Handbook for X-ray Photoelectron Spectroscopy*, Physical Electronics Inc., Chanhassen, Minnesota USA, 1995.

[53] E. Csiszar, E. Fekete, *Langmuir* 27 (2011) 8444–8450.

[54] W.P. Davey, *Phys. Rev.* 25 (1925) 753–761.

[55] H. Köhlmann, C. Ritter, AZ. Anorg. Alg. Chem. 635 (2009) 1573–1579.

[56] F.A. Marchesini, S. Irusta, C. Querini, E. Miró, *A. Appl. Catal.* 348 (2008) 60–70.

[57] J. Zhao, W. Li, D. Fang, *RSC Adv.* 5 (2015) 42861–42868.

[58] C. Zhang, S.N. Oliaee, S.Y. Hwang, X. Kong, Z. Peng, *Nano Lett.* 16 (2015) 164–169.

[59] Y. Kitamura, A. Tanaka, M. Sato, K. Oono, T. Ikawa, T. Maegawa, Y. Monguchi, H. Sajiki, *Synth. Commun.* 37 (2007) 4381–4388.

[60] L. Lemaignen, C. Tong, V. Begon, R. Burch, D. Chadwick, *Catal. Today* 75 (2002) 43–48.

[61] F.A. Marchesini, L.B. Gutierrez, C.A. Querini, E.E. Miró, *J. Chem. Eng.* 159 (2010) 203–211.

[62] N. Krawczyk, I. Witonska, A. Krolak, M. Frajtak, S. Karski, *Rev. Roum. Chim.* 56 (2011) 595–600.

[63] R.W. Hewitt, N. Winograd, *J. Appl. Phys.* 51 (1980) 2620–2624.

[64] S. Lany, A. Zakutayev, T.O. Mason, J.F. Wager, K.R. Poeppelmeier, J.D. Perkins, J.J. Berry, D.X. Ginley, A. Zunger, *Phys. Rev. Lett.* 108 (2012) 016802.

[65] J.I. Jeong, J.H. Moon, J.H. Kong, J.S. Kang, Y.P. Lee, *Appl. Phys. Lett.* 64 (1994) 1215–1217.

[66] G.J. Exarhos, X.-D. Zhou, *Thin Solid Films* 515 (2007) 7025–7052.

[67] J.R. Rumble (Ed.), *Properties of Solids* in CRC Handbook of Chemistry and Physics, 98th Edition (Internet Version 2018), CRC Press/Taylor & Francis, Boca Raton, FL, 2017.

[68] B.P. Chaplin, J.R. Shapley, C.J. Werth, *Environ. Sci. Technol.* 41 (2007) 5491–5497.

[69] B.P. Chaplin, J.R. Shapley, C.J. Werth, *Catal. Lett.* 130 (2009) 56–62.

[70] M. D'Arino, F. Pinna, G. Strukul, *Appl. Catal. B* 53 (2004) 161–168.

[71] S. Ambonguilat, H. Gallard, A. Garron, F. Epron, J.P. Croue, *Water Res.* 40 (2006) 675–682.

[72] A. Pintar, J. Batista, J. Levec, *Catal. Today* 66 (2001) 503–510.

[73] A.J. Bard, L.R. Faulkner, *Electrochemical Methods, Fundamentals and Applications*, 2nd edition, John Wiley & Sons, Ltd, Hoboken New Jersey, 2001.

[74] J. Buha, I. Djerdj, M. Neiederberger, *Cryst. Growth Des.* 7 (2006) 113–116.

[75] N.N. Greenwood, A. Earnshaw, *Chemistry of the Elements (2nd Edition)*, Reed Educational and Professional Publishing, Great Britain, 1997.

[76] F.A. Cotton, G. Wilkinson, P.L. Gaus, *Basic Inorganic Chemistry*, 3rd edition, Wiley, New York, 1995.

[77] K. Wade, A.J. Banister, *The Chemistry of Aluminium, Gallium, Indium, and Thallium, Comprehensive Inorganic Chemistry*, Pergamon Press, New York, 1975.

[78] T.L. Amyes, S.T. Diver, J.P. Richard, F.M. Rivas, K. Toth, *J. Am. Chem. Soc.* 126 (2004) 4366–4374.

[79] P. Wasserscheid, T. Welton, *Ionic Liquids in Synthesis*, Wiley-VCH, Germany, 2008.

[80] O. Holloczki, D. Gerhard, K. Massone, L. Szarvas, B. Nemeth, T. Veszpremi, L. Nyulaszi, *New J. Chem.* 34 (2010) 3004–3009.

[81] B.P. Chaplin, E. Roundy, K.A. Guy, J.R. Shapley, C.J. Werth, *Environ. Sci. Technol.* 40 (2006) 3075–3081.

[82] C.A. Crock, V.V. Tarabara, *Environ. Sci.: Nano* 3 (2016) 453–461.